HHS Public Access

Author manuscript

Mutat Res. Author manuscript; available in PMC 2017 August 01.

Published in final edited form as:

Mutat Res. 2016 August ; 790: 8–18. doi:10.1016/j.mrfmmm.2016.05.005.

Site-directed mutants of human RECQ1 reveal functional importance of the zinc binding domain

Furqan Sami[1], **Ronald K. Gary**[2], **Yayin Fang**[1], and **Sudha Sharma**[1,*]

[1]Department of Biochemistry and Molecular Biology, College of Medicine, Howard University, 520 W Street, NW, Washington, DC 20059, USA

[2]Department of Chemistry and Biochemistry, University of Nevada, Las Vegas, 4505 Maryland Parkway, Las Vegas, NV 89154-4003, USA

Abstract

RecQ helicases are a highly conserved family of ATP-dependent DNA-unwinding enzymes with key roles in DNA replication and repair in all kingdoms of life. The RECQ1 gene encodes the most abundant RecQ homolog in humans. Mutations in RECQ1 significantly increase breast cancer susceptibility. We engineered full-length RECQ1 harboring point mutations in the zinc-binding motif (amino acids 419–480) within the conserved RecQ-specific-C-terminal (RQC) domain known to be critical for diverse biochemical and cellular functions of RecQ helicases. Wild-type RECQ1 contains a zinc ion. Substitution of three of the four conserved cysteine residues that coordinate zinc severely impaired the ATPase and DNA unwinding activities but retained DNA binding and single strand DNA annealing activities. Furthermore, alteration of these residues attenuated zinc binding and significantly changed the overall conformation of full-length RECQ1 protein. In contrast, substitution of cysteine residue at position 471 resulted in a wild-type like RECQ1 protein. Differential contribution of the conserved cysteine residues to the structure and functions of the RECQ1 protein is also inferred by homology modeling. Overall, our results indicate that the zinc binding motif in the RQC domain of RECQ1 is a key structural element that is essential for the structure-functions of RECQ1. Given the recent association of RECQ1 mutations with breast cancer, these observations will contribute to understanding the molecular basis of RECQ1 functions in cancer etiology.

Keywords

RecQ; helicase; zinc-binding domain; mutation; strand-annealing

*Correspondence should be addressed to: Sudha Sharma Howard University College of Medicine Department of Biochemistry and Molecular Biology 520 W St. NW, Washington, DC 20059, USA. Tel.: 202-806-9750; fax: 202-806-5784.

Conflict of interest

The authors declare that there is no conflict of interest.

1. INTRODUCTION

RECQ1, also known as RECQL or RECQL1, is the most abundant member of the highly conserved RecQ family of DNA helicases implicated in genome maintenance and represented by five homologs in humans: RECQ1, BLM, WRN, RECQL4, and RECQL5 [1]. Mutations in three of five RecQ genes, *BLM, WRN* and *RECQl4* are associated with rare genetic diseases of cancer predisposition and/or premature aging [2,3]. Within the last year, whole genome sequencing efforts have revealed that missense mutations in *RECQ1* gene predispose individuals to familial breast cancer [4,5]. Thus, *RECQ1* is now classified as a breast cancer susceptibility gene [6]. We and others have demonstrated that the loss of RECQ1 causes genomic instability [7]. Cells lacking RECQ1 have a higher rate of spontaneous sister chromatid exchange, are more sensitive to genotoxins, and undergo more double-stranded DNA breaks [8–12]. RECQ1 seems to prevent such DNA breaks by stabilizing stalled or regressed replication forks [13–15]. In addition, RECQ1 is involved in non-homologous end joining [16] and lengthening of telomeres without telomerase [17]. Altogether, this suggests that RECQ1 has a tumor-suppressor role.

RECQ1 protein (649 amino acid residues) contains a highly conserved core helicase domain, the RecQ-specific C-terminal (RQC) domain and short N and C termini extensions [18]. RECQ1, however, lacks HRDC domain present in several RecQ proteins including bacterial RecQ and human WRN and BLM proteins [19]. Biochemically, RECQ1 participates in the processing of DNA structure intermediates of replication and repair by catalyzing ATP-dependent 3’–5’ unwinding of a variety of duplex DNA substrates and promoting branch migration of Holliday junction and D-loops[7,20–22]. Moreover, RECQ1 supports base-pairing of complementary single strand DNA in an ATP-independent manner [7,20–22]. Different activities of RECQ1 are associated with distinct assembly states; a monomer or dimer form for DNA unwinding and a higher-order form (hexamer or pentamer) for strand annealing activities [23,24]. ATP-binding governs the oligomeric status, and consequently biochemical activities, of RECQ1 and promotes the smaller oligomeric form capable of duplex unwinding [21,23]. Investigating how the mutations in RECQ1 alter the protein’s oligomerization or ligand binding properties and affect its catalytic activities will help to understand critical functions of RECQ1 necessary for its biological activity in vivo.

The crystal structure of a truncated RECQ1, containing 49–619 amino acids, resembles that of *E. coli* RecQ and exhibits four structurally defined domains: two RecA-like domains (D1 and D2) containing the widely conserved helicase/ATPase motifs with the nucleotide-binding site located between these two domains (PDB ID code 2V1X) and two separately folded domains, a zinc-binding domain (ZBD) and a winged-helix (WH) domain comprising the signature RQC domain of RecQ family [25]. The ATPase and RQC domains generally comprise a “helicase core” of the RecQ family [26]. Helicase domain is believed to mediate nucleotide-binding and translocation, but the accessory domains are expected to be equally significant in structure and functions of RECQ1. Substitution of two invariant aromatic loop residues, W227 and F231, located within the conserved aromatic-rich sequence between motifs II and III of helicase core of full-length RECQ1 with alanine resulted in abrogation of helicase and branch migration activities but retention of DNA binding, oligomerization, ATPase, and strand annealing [27]. A unique tyrosine residue (Y564), at the tip of the β-

hairpin motif which forms a wing of the WH domain, controls the activity of RECQ1 to unwind a simple fork duplex without impacting single strand DNA-dependent ATPase activity [25]. Mutations of the double strand DNA binding residues T511, K514, and R528 in the WH domain in the full-length protein adversely impacted DNA helicase activity but retained the strand annealing function of RECQ1[22]. An isolated WH domain (amino acids 481–624) of RECQ1 displayed similar strand annealing activity as the full-length tetrameric RECQ1. Contrary to this, a longer protein fragment spanning D2-ZBD-WH domains (amino acids 282–624) completely lacked strand annealing activity [22]. These studies suggest additional structural features that contribute to the catalytic functions and the overall conformational state of the RECQ1 protein.

The WH of RECQ1 interacts with significantly different regions of its core helicase and zinc-binding domains as compared to those of *E. coli* RecQ and the human WRN protein [25]. The RECQ1 crystal structure indicates that in the ZBD (amino acids 419–480), the zinc ion is coordinated by the side chains of four cysteine residues located on two antiparallel α-helices (Figure 1). The ZBD of *E. coli* RecQ [28] as well as the human BLM [29,30], WRN [31], and RECQL5 [32] is important for protein structure and functions. Here, we investigated the contribution of RECQ1 ZBD to the catalytic activities by using site-directed point mutants of conserved cysteine residues in full-length RECQ1.

2. MATERIALS AND METHODS

2.1. Site-directed mutagenesis

PCR-based site-directed mutagenesis (the QuikChange site-directed mutagenesis kit, Stratagene, La Jolla, CA) was used for the generation of pET28 RECQ1 constructs having alanine instead of cysteine at amino acid position 453, 471, 475 or 478 following the manufacturer's instructions. The constructs were verified by DNA sequencing.

2.2. Expression and purification of the proteins

Competent *E. coli* strain BL21-CodonPlus (DE3)-RIPL (Agilent Technologies) cells were transformed with pET28 (a+) plasmids encoding the wild-type, C453A, C471A, C475A and C478A mutants. Transformed colony was grown overnight at 37°C in 10 mL of TB medium (1% tryptone, 0.5% yeast extract, 0.5% NaCl) and 50 μg/mL kanamycin. One percent overnight culture was used to seed TB medium, including 50 μg/mL kanamycin and 20 mL of ethanol and grown at 37°C to OD_{600} = 3.0 followed by IPTG (1 mM) induction overnight at 18°C. Bacterial culture was centrifuged at 8,000g for 10 min, washed in 50 mL of ice-cold PBS, and resuspended in lysis buffer (50 mM HEPES-KOH (pH 7.5), 0.5 M NaCl, 5% glycerol, 1 mg/mL lysozyme (Promega), 10 mM imidazole, 1 mM TCEP supplemented with protease inhibitor (Roche) and benzonase (Novagen)) and frozen at −80°C. Frozen bacterial lysate was thawed on ice, extracted by sonication pulses (8 × 10 sec) and centrifuged at 16,000g for 30 min. Subsequently, 0.1% polyethyleneimine solution (pH 7.5) was added to remove nucleic acids and cell debris by centrifugation at 16,000g for 60 min. The clarified supernatant was filtered through 0.45 μM PES membrane and then loaded on 5 mL HiTrap TALON® crude column (GE Healthcare) at 1 mL/min by using AKTA purifier system. The column was washed 10 times with wash buffer (50 mM HEPES (pH 7.5), 0.5 M NaCl, 5%

glycerol, 30 mM imidazole) and eluted with elution buffer (50 mM HEPES (pH 7.5), 0.5 M NaCl, 5% glycerol, 250 mM imidazole, 1 mM TCEP). Protein from TALON pools was concentrated by ammonium sulfate precipitation (80% saturation), resuspended in storage buffer and desalted overnight using 10,000 MWCO Slide-A-Lyzer® dialysis cassettes (Thermo Scientific). Purified recombinant proteins judged to be > 95% pure from analysis on Coomassie-stained SDS polyacrylamide gels were frozen in liquid nitrogen and stored at −80°C. The protein concentrations were determined by the Bio-Rad DC Protein Assay.

2.3. DNA substrates

PAGE-purified oligonucleotides used for preparation of DNA substrates were purchased from Midland Certified Reagent Co. 5′-^{32}P-Labeled duplex DNA substrates were prepared as described previously [21]. Oligonucleotide sequences are indicated in Table 1.

2.4. DNA helicase assay

Helicase reaction mixtures (20 μL) containing 20 mM Tris-HCl (pH 7.5), 10 mM KCl, 8 mM dithiothreitol (DTT), 5 mM $MgCl_2$, 5 mM ATP, 10% glycerol, 80 μg/mL BSA and 0.5 nM radiolabeled DNA substrate were initiated by adding indicated RECQ1 concentrations. Reactions were incubated for 30 min at 37°C, followed by the addition of 20 μL of stop buffer (35 mM EDTA, 0.6% SDS, 25% glycerol, 3 mg/ml proteinase K, 0.04% bromophenol blue, and 0.04% xylene cyanol) with a 10-fold molar excess of unlabeled competitor oligonucleotide to prevent re-annealing of the unwound single strand DNA products. Reaction products were subsequently resolved on non-denaturing 12% polyacrylamide gels. Radiolabeled DNA species on polyacrylamide gels were visualized with a PhosphorImager and quantitated using ImageQuant software (Amersham Biosciences).

2.5. ATP hydrolysis assay

ATP hydrolysis was measured using [γ-^{32}P] ATP (PerkinElmer Life Sciences) by thin layer chromatography (TLC) on polyethyleneimine-cellulose plates (JT Baker). The standard reaction mixture (20 μL) contained 40 mM Tris-HCl (pH 7.4), 25 mM KCl, 5 mM $MgCl_2$, 2 mM DTT, 2% glycerol, 100 μg/mL BSA, $(dT)_{40}$ oligonucleotide as single strand DNA effector (32 μM nucleotide), and 250 μM [γ-^{32}P]ATP, with indicated concentration of RECQ1 wild-type and mutant proteins. Reactions were incubated for 30 min at 30°C. Reaction mixtures were resolved onto a TLC plate by using 0.5 M LiCl, 1 M formic acid as the carrier solvent, visualized using a PhosphorImager and analyzed with ImageQuant software.

2.6. ATP binding assay

We used a previously described UV cross-linking protocol [33] to assess the ATP binding ability of wild-type and the mutant RECQ1 proteins. Briefly, 1 μg RECQ1 proteins were premixed in 10 μL of ATP-binding buffer (20 mM HEPES-KOH (pH 7.5) and 5 mM magnesium acetate) for 15 min on ice. Then 2.5 μCi (2pmol) of [γ-^{32}P] ATP and 180 pmol of cold ATP were added to the pre-incubated proteins. Reaction mixtures were incubated on ice for 15 min followed by irradiation using a UV cross-linker (254 nm, UVP CL-1000) situated at a distance of 5 cm for 10 min. Samples were boiled in sample buffer for 5 min

and separated by SDS-PAGE. The gels were stained with Coomassie blue and visualized using a PhosphorImager.

2.7. DNA strand annealing assay

The strand annealing activity of RECQ1 was measured using partially or fully complementary synthetic oligonucleotides (each at a concentration of 0.5 nM), labeled at the 5′-end using [γ-^{32}P] ATP and T4 polynucleotide kinase. Reactions (20 μL) were carried out in helicase reaction buffer in the absence of ATP and contained the indicated RECQ1 concentrations. Reactions were initiated by the addition of the unlabeled DNA strand, followed by incubation for 30 min at 37°C. A control reaction mixture was set up in an identical manner to determine the level of spontaneous annealing of oligonucleotides in the absence of RECQ1. Reactions were terminated by the addition of 20 μL of stop buffer followed by incubation with proteinase K (0.1 mg/mL) for 15 min at 37°C, and the products were resolved on native 12% polyacrylamide gels. Radiolabeled DNA species on polyacrylamide gels were visualized with a PhosphorImager and quantitated using ImageQuant software.

2.8. DNA binding assay

The binding assay took advantage of a high binding affinity between streptavidin-conjugated agarose beads (M-280 Streptavidin Dynabeads (Invitrogen)) and biotinylated DNA which allows for pulling down DNA-bound proteins as we have described previously [16]. Briefly, wild-type or mutant RECQ1 protein (100 nM) was allowed to incubate with biotinylated DNA (60 ng) in 40 μL of binding buffer (25 mM Tris HCl (pH 7.5), 150 mM KCl, 100 μg/mL BSA, 5% glycerol, 0.1% Triton X100 and 2 mM DTT) at room temperature for 20 min, and subsequently incubated with 20 μL of pre-washed Dynabeads for 15 min at room temperature. Supernatant was discarded, and the beads were resuspended in 0.2 mL of washing buffer (binding buffer minus glycerol) and the suspension was split in halves for DNA and protein analyses following three washes. Proteins were eluted from the beads in 20 μL of 2× SDS-sample at 90°C for 5 min and analyzed by Western blotting with anti-RECQ1 antibody. DNA was eluted in 20 μL of 10 mM EDTA (pH 8.2) with 95% formamide at 90°C for 1 min, run on 2% TAE agarose gel and stained with EtBr.

2.9. Microscale thermophoresis

Microscale thermophoresis (MST) was used to measure the dissociation constant for the interaction of wild-type or mutant RECQ1 proteins with a forked duplex DNA substrate. The DNA consisted of 5'-fluorescein-labeled T44 oligo annealed to unlabeled FLAP26 oligo. The MST binding buffer was 25 mM Tris-HCl at pH 8.0, 25 mM NaCl, 2 mM $MgCl_2$, 5% glycerol, 1 mM DTT, 0.1% Tween-20, 0.1 mg/ml BSA. DNA was diluted in MST binding buffer to give a final concentration of 20 nM, and protein stocks in storage buffer (50 mM Tris-HCl at pH 8.0, 100 mM NaCl, 10% glycerol, 1 mM DTT) were diluted first with an equal volume of water and then subject to 2-fold serial dilution with MST binding buffer to give a 16 point series at the indicated final concentrations. One-half strength storage buffer is highly similar to MST binding buffer, but it is not identical; control experiments demonstrated that buffer constituents did not alter MST performance under the conditions employed. DNA/protein mixtures were loaded into capillary tubes and analyzed

on a Monolith NT.115 (NanoTemper Technologies) with the IR laser set at 60% power. The T-jump signal was converted to normalized fluorescence (F_{norm}) and MO.Affinity Analysis software was used to fit a non-cooperative model binding curve to the data and calculate a K_d value with 68% confidence interval.

2.10. Differential scanning fluorimetry

Differential scanning fluorimetry was set up in 96 well PCR plates using a reaction volume of 100 μL as described previously [34]. Reaction mixtures contained wild-type or mutant RECQ1 (10 μM), 6 mM $MgCl_2$, 50 mM HEPES (pH 8.0), 80 mM NaCl, 5.25% glycerol (v/v) and 1.4X SYPRO Orange (Invitrogen) in the presence or absence of 5 mM ATP. Two controls with eight repetitions per plate were used for the thermal shift experiments: 0.5% DMSO; 0.5 mM ATP, 0.5% DMSO. Differential fluorimetric scans were performed in a real-time PCR machine (CFX96 real-time PCR system (Bio-Rad)) using a temperature scan from 25°C to 90°C at 0.5°C/min and data were exported to Excel for analysis.

2.11. Quantification of zinc ion bound to RECQ1 proteins

The zinc content of the wild-type and the cysteine mutants of RECQ1 helicase was measured by the 4-(2-Pyridylazo)resorcinol (PAR) assay as reported earlier [35]. PAR has a low absorbance at 500 nm in the absence of zinc ion. However, in the presence of zinc ion, the absorbance at 500 nm increases dramatically due to the formation of the PAR_2·zinc complex. All the buffers were pre-treated with Chelex 100 resin to remove any traces of zinc that might be present, thus enabling precise quantification of the zinc content of wild-type and mutant RECQ1 proteins. The proteins were dialyzed and reconcentrated on Amicon Ultra-0.5 mL centrifugal filters against EDTA-free Chelex-treated buffer (passed over a 10-cm column of Chelex-100). Twenty μL (approximately 1 nmol) dialyzed protein was denatured with Chelex-treated 7 M guanidine HCl and then transferred to a 1 mL cuvette. Volume was adjusted to 0.9 mL with buffer A (20 mM Tris-HCl (pH 8.0) and 150 mM NaCl) followed by the addition of PAR into the cuvette for a final concentration of 100 μM. The absorbance was recorded from 300 to 600 nm at 25°C via a SPECTROstar Nano microplate reader (BMG Labtech Inc). The quantity of zinc ion was measured using the absorbance coefficient for the $(PAR)_2$-zinc complex ($\varepsilon_{500} = 6.6 \times 10^4\ M^{-1}\ cm^{-1}$). As a control, a solution of 20 μM pure $ZnCl_2$ was quantified in the same reaction condition.

2.12. Limited proteolytic digestion

The wild-type, mutant, and zinc ion extracted RecQ helicases at a concentration of 15 μM and in a total volume of 30 μL were digested with α-chymotrypsin (Sigma) for 15 min at room temperature. The ratio between the protease and substrate was 1:100 for each protein. Aliquots (15 μL corresponding to 1 μg of protein) from the reaction were quenched with 15 μL of gel-loading buffer (250 mM Tris-HCl (pH 6.8), 3.4% SDS, 1.1 M 2-mercaptoethanol, 20% glycerol, and 0.01% bromophenol blue). The samples were boiled for 5 min, resolved by SDS-PAGE and stained with Coomassie blue.

3. RESULTS

Amino acid sequence alignment of the ZBD among the RecQ family helicases identified conserved cysteine residues at position 453, 471, 475 and 478 in RECQ1 (Figure 1). Full-length RECQ1 proteins, wild-type (RECQ1-WT) or with engineered single amino acid substitutions with alanine at conserved cysteine residues (RECQ1-C453A, RECQ1-C471A, RECQ1-C475A, and RECQ1-C478A) were overexpressed in bacteria and purified to near homogeneity using a previously reported method [25,36].

3.1. Effects of the mutations on DNA unwinding activity

We first compared the helicase activities of the wild-type and mutant RECQ1 proteins using its preferred substrate, a fork duplex with 5’ and 3’ single strand DNA arms [21]. Standard helicase assay using increasing concentrations (0.312–160 nM) of recombinant RECQ1 proteins demonstrated that substitution of the cysteine residue at 453, 475 or 478 to alanine abolished the ability of RECQ1 to unwind a 19-bp forked duplex which was efficiently unwound by the wild-type RECQ1 (Figure 2A, 2B). In contrast, RECQ1-C471A mutant unwound the forked duplex with a similar efficiency as the wild-type RECQ1 over the range of protein concentration tested (Figure 2A and 2B). Approximately 40% of the fork duplex was unwound by 2.5 nM RECQ1-WT or RECQ1-C471A and > 80% unwinding was achieved by 20 nM RECQ1-WT or RECQ1-C471A mutant (Figure 2A and 2B). Notably, RECQ1-C453A, RECQ1-C475A, and RECQ1-C478A mutants failed to unwind fork duplex and no detectable unwinding of the fork duplex was observed even at the excessively increased protein concentration (160 nM) (Figure 2A and 2B). Consistent with their inability to unwind fork duplex, RECQ1 variants RECQ1-C453A, RECQ1-C475A and RECQ1-C478A failed to unwind a 5’-flap substrate that mimics intermediate of DNA replication and repair and is unwound by wild-type RECQ1 [21,36]. In a control reaction and as previously reported [21], RECQ1 protein containing a K119A mutation within the helicase domain also failed to unwind 5’-flap DNA substrate. In contrast, nearly the same percent of the 5’-flap substrate was unwound by RECQ1-WT and RECQ1-C471A at the tested protein concentrations (20 nM and 40 nM) (Figure 2C). These results suggest that RECQ1-C471A variant retains helicase activity on both forked duplex and 5’-flap DNA substrates whereas substitution of cysteine 453, 475 or 478 to alanine abolishes the helicase activity of RECQ1.

3.2. Effect of the mutations on ATP hydrolysis and binding

To determine the role of ZBD in ATP hydrolysis, we compared the single strand DNA-dependent ATPase activities of the cysteine mutants with the wild-type RECQ1 helicase (Figure 3). The amount of ATP hydrolysis in the presence of single strand DNA (40-mer) was monitored by thin layer chromatography as we have previously reported [37]. Figure 3A shows the cleavage of labeled phosphate (top band) from ATP (bottom band) by wild-type RECQ1 and RECQ1-ZBD mutant proteins in the presence of a fixed amount of single strand DNA effector (Figure 3A). Plotting the data revealed a pattern of ATPase activity similar to that observed for helicase activity (Figure 3B) A comparable fraction of ATP-hydrolysis was observed for RECQ1-WT and RECQ1-C471A proteins over the range of protein concentration tested (5, 10 and 20 nM) (Figure 3A and 3B). In contrast, RECQ1-C453A, RECQ1-C475A and RECQ1-C478A did not exhibit ATP hydrolysis (Figure 3A and 3B).

Thus, the ZBD mutants of RECQ1 that are helicase deficient are also defective in hydrolyzing ATP.

We next studied the ATP binding to the mutant RECQ1 proteins. Wild-type and mutant RECQ1 proteins were incubated with a mixture of [γ-^{32}P] ATP and cold ATP, and subsequently UV cross-linked. Proteins that display ATP binding activity would become covalently linked to ATP and thus be radiolabelled. Phosphorimage analysis demonstrated that both RECQ1-WT and RECQ1-C471A proteins were efficiently labeled whereas RECQ1-C453A, RECQ1-C475A and RECQ1-C478A variants did not bind ATP (Figure 3C). In control reactions, the RECQ1-K119A protein in which the conserved lysine residue of the Walker A box (motif I) implicated in ATP binding is mutated, were also unlabeled [38]. No radioactive signal was observed for the controls where reaction mixture containing RECQ1-WT was not exposed to UV (designated as WT-UV) or if BSA was used in place of the RECQ1 proteins. Notably, using the same assay, substitution of conserved cysteine residues to asparagine was shown to not affect the ATP binding activity of BLM protein [29]. Thus, substitution of cysteine with alanine at positions 453, 475, or 478 within the ZBD of RECQ1 disrupts ATP binding, ATP hydrolysis and DNA duplex unwinding activities of RECQ1. Remarkably, RECQ1 variant with C471A substitution retains ATP binding, ATP hydrolysis and unwinding at a level comparable to that demonstrated by the wild-type RECQ1 in vitro.

3.3. Effect of the mutations on DNA annealing activity

To analyze strand annealing activity of the RECQ1 ZBD mutants, we incubated two partially complementary single-strand oligonucleotides with increasing concentrations of purified recombinant RECQ1-WT or RECQ1-ZBD mutant proteins in the absence of ATP and analyzed the products on native polyacrylamide gels. Both wild-type and ZBD-mutant RECQ1 proteins promoted annealing of the partially complementary strands in a protein concentration dependent manner (Figure 4B). Compared to the wild-type protein, RECQ1 mutants C453A, C475A and C478A promoted significantly greater strand-annealing to form the splayed arm duplex, which co-migrated with the intact forked duplex control; in contrast, strand-annealing by RECQ1-C471A was comparable to RECQ1-WT (Figure 4A and 4B). At 1.25 nM, RECQ1-WT promoted 38% annealing whereas RECQ1-C453A, RECQ1-C471A, RECQ1-C475A and RECQ1-C478A promoted 53, 35, 54, and 71% annealing, respectively and DNA strand-annealing achieved a plateau at higher (10 nM) RECQ1 protein in the reaction (Figure 4B).

We next performed similar experiments using fully complementary oligonucleotides that generate a 44-bp blunt duplex product upon annealing. Consistent with the results on partial duplex, the RECQ1 ZBD mutants C453A, C475A and C478A supported significantly greater strand-annealing as compared to RECQ1-WT, whereas the RECQ1-C471A mutant behaved similar to the wild-type RECQ1 (Figure 4C). As we have shown previously, RECQ1-K119A retained its ability to catalyze strand-annealing comparable with the wild-type RECQ1 protein (Figure 4C).

The biological significance of the strand-annealing activities of helicases is yet to be understood; however it has been proposed that the coordinated action of unwinding and

annealing by RECQ1 and other helicases may play a role in fork regression or synthesis-dependent strand-annealing, in the pathway for double strand break repair, as well as in transcription and telomere metabolism [39]. The helicase and strand-annealing activities of RECQ1 are modulated by the nature of the DNA substrate, availability of ATP, and the interacting protein partners [21]. In this study, we have only characterized the helicase and strand-annealing activity of RECQ1-ZBD mutants. It will be insightful to test, in future, the ability of these mutants for the branch migration of Holiday Junctions and D-loops which involves both helicase and strand-annealing activities [22].

3.4. Folding properties of RECQ1 cysteine mutants

Zinc binding domain has also been implicated in RecQ protein stability [28,32]. Using differential scanning fluorimetry, we tested the stability of the RECQ1-WT and RECQ1-ZBD proteins in the absence and presence of ATP. As compared to RECQ1-WT which exhibits a thermal transition at 46°C, RECQ1-C471A mutant showed a relatively similar thermal transition of 47°C. However, RECQ1-C453A, RECQ1-C475A and RECQ1-C478A displayed an enhanced thermo-instability as suggested by their lower T_m values than the RECQ1-WT (Figure 5A). Thermal shift assays performed in the presence of 5 mM ATP yielded T_m values of 52°C for RECQ1-WT and RECQ1-C471A indicating that ATP binding rendered stability to these proteins; however, RECQ1-C453A, RECQ1-C475A, and RECQ1-C478A exhibited a minimal thermal shift with addition of ATP, indicating lack of ATP binding (Figure 5B). Together, these data show that the RECQ1-C471A mutant maintains similar structural stability as RECQ1-WT, while replacing single cysteine residues at positions 453, 475 or 478 likely precludes the acquisition of a wild-type conformation.

3.5. Quantification of zinc bound to wild-type RECQ1 and RECQ1-ZBD mutant proteins

We examined the zinc binding ability of the wild-type and RECQ1-ZBD mutant proteins using PAR, a reporter dye that absorbs light at approximately 500 nm when bound to zinc [35]. The proteins were dialyzed against zinc-free buffer, and then denatured to release protein-associated zinc and make it available for interaction with PAR. As shown in Figure 6A, the increase in PAR absorbance at 500 nm following addition of RECQ1-WT or RECQ1-C471A indicates that these proteins contained zinc. In contrast, significantly lower absorbance following the addition of RECQ1-C453A, RECQ1-C475A and RECQ1-C478A to PAR solution shows that these mutants lack protein-associated zinc (Figure 6A). Quantitative analysis of the zinc associated with the purified RECQ1-WT and RECQ1-C471A proteins indicated that the zinc atom binds to the proteins in a 1:1 stoichiometric ratio. This observation was further confirmed by the existence of a linear correlation between the amount of zinc ion and the increasing concentration of the protein (Figure 6B). The slope value of 0.99 ± 0.12 indicates that each molecule of RECQ1 contains one zinc ion. The RECQ1-K119A binds zinc same as RECQ1-WT and RECQ1-C471A. In contrast, the zinc content of the RECQ1-C453A, RECQ1-C475A and RECQ1-C478 mutants appeared to be only 0.12–0.24 mol/mol enzyme.

To determine whether zinc stabilizes the conformation of RECQ1 that might be responsible for its effect on RECQ1's biochemical activities, we performed limited proteolysis of wild-type RECQ1 and RECQ1-ZBD mutants (Figure 6C). RECQ1 was digested by chymotrypsin

in a 10min reaction, yielding a characteristic pattern of RECQ1 proteolytic fragments (Figure 6C, lane 3). We also examined the proteolytic pattern of zinc-demetalated RECQ1 in which the zinc atom was removed from the wild-type RECQ1 by EDTA extraction (Figure 6C, lane 4). Upon chymotrypsin digestion, the proteolysis pattern of zinc-demetalated RECQ1-WT was markedly different from that of zinc-metalated RECQ1-WT (Figure 6C, lanes 3 and 4). The proteolysis pattern of RECQ1-C453A, RECQ1-C475A, and RECQ1-C478A closely resembled that of zinc-demetalated RECQ1-WT (Figure 6C, lanes 6, 10 and 12); whereas RECQ1-C471A was hydrolyzed in a manner similar to zinc-metalated RECQ1-WT upon chymotrypsin digestion (Figure 6C, lane 8). These results suggest that zinc ion is critical for the three dimensional structure of wild-type RECQ1, and the RECQ1-C453A, RECQ1-C475A, and RECQ1-C478A mutants that lack zinc assume different conformation(s).

3.6. DNA binding activity of RECQ1-ZBD cysteine mutants

To confirm that wild-type RECQ1 and RECQ1-ZBD mutants could bind to the DNA duplex, we first used a 322 bp biotinylated DNA probe in binding reaction containing wild-type or mutant RECQ1 proteins. The DNA-protein complexes were pulled down using streptavidin magnetic beads and DNA-bound RECQ1 was detected by Western blot (Figure 7A, upper panel). Quantitative analysis of the Western blot indicated that as compared to the wild-type RECQ1 protein, the cysteine to alanine substitution at positions 453, 475 or 478 resulted in RECQ1 variants with significantly enhanced ability to bind DNA duplex. In contrast, the RECQ1-C471A mutant retained only about 40% DNA binding activity of the RECQ1-WT (Figure 7B).

To compare the relative affinities of the wild-type and mutant proteins to bind the fork duplex DNA substrate, and to measure the absolute value of dissociation constants (K_d), we employed MST assay. The wild-type RECQ1 protein and each of the four RECQ1-ZBD cysteine mutants were observed to interact with fluorescently-labeled forked duplex DNA (Figure 8). A control MST run, using 2-fold serial dilutions of storage buffer with no protein, demonstrated that buffer constituents have no effect on the MST signal (Figure 8). A K_d of 66 nM was observed for the interaction of wild-type RECQ1 with forked duplex DNA. The zinc-binding mutant RECQ1-C471A also produced a concentration-dependent change in the thermophoretic behavior of the DNA, but only the two highest concentrations available produced significant binding and this was insufficient for delineation of a binding curve. For the C471A mutant, the available data indicate a K_d of approximately 1000 nM or higher in this assay. In comparing the two zinc-containing proteins, RECQ1-WT and RECQ1-C471A, superior DNA binding by the wild-type was observed in the pull-down assay (Figure 7) and also in the MST assay (Figure 8). For the three mutants that cannot bind zinc (RECQ1-C453A, RECQ1-C475A, and RECQ1-C478A), the K_d values for DNA interaction were 276, 473, and 602 nM, respectively (Figure 8B). Thus, both the pull-down assay and the MST assay show that the three RECQ1 mutants that lack zinc bind to DNA better than the RECQ1-C471A mutant that contains zinc.

We note that the RECQ1-WT protein displayed the strongest binding to fork-duplex in MST assay; whereas the pull-down assay using a blunt duplex suggested that the zinc-defective

mutants bind to DNA even better than wild-type protein. This disparity could be due to differences in the nature of the DNA substrate used (a 322 bp dsDNA in the pull-down assay versus a 19 bp forked structure in the MST assay), differences in free versus immobilized binding format, or other aspects that differentiate the two approaches. The fork duplex substrate used in the MST assay possesses structurally-distinct potential binding sites: single-stranded DNA, duplex DNA, and a fork junction; and presumably, each region of DNA may have a different affinity for DNA-binding proteins. The observed MST behavior and the resulting K_d is expected to represent a composite of the different types of binding events that may be possible [40].

4. DISCUSSION

RECQ1 functions are critical for genome maintenance [7,41]. We engineered full-length RECQ1 harboring point mutations in the ZBD (amino acids 419–480) within the conserved RQC domain to determine critical amino acid residues that determine its catalytic activities and thus may dictate cellular functions. Substitution with alanine of three of the four conserved cysteine residues (C453A, C471A, C475A and C478A) that coordinate zinc binding resulted in substantial loss of unwinding activity except for C471A indicating differential contribution to catalytic function of RECQ1. We confirmed that RECQ1-C453A, RECQ1-C475A and RECQ1-C478A are deficient in ATP hydrolysis and functionally helicase-dead, and fail to unwind fork duplex even at 10-fold higher concentration than what is required for maximum unwinding by the RECQ1-WT or RECQ1-C471A protein. Conversely, RECQ1-C453A, RECQ1-C475A and RECQ1-C478A variants exhibited robust DNA binding and annealing of single strand DNA. Heat denaturation analysis of both wild-type and mutant RECQ1 proteins revealed that alteration of cysteine residues 453, 475 or 478 change the overall conformation of full-length RECQ1 protein. Overall, this study highlights the importance of ZBD to the structure and functions of RECQ1 protein and illustrates distinct roles of individual conserved cysteine residues in coordinating zinc ion in the ZBD.

Previously, alterations in the ZBD of RECQ1's structural homolog *E.coli* RecQ protein resulted in a complete loss of DNA binding [28]. A remarkable observation in our study is that the alteration of the ZBD by substitution of conserved cysteine residues at positions 453, 475, and 478 with alanine retained DNA binding ability. Recently solved crystal structures of human RECQ1 helicase in complexes with tailed-duplex DNA and single strand DNA reveals a direct contact of ZBD to the 3'single strand DNA tail via residue M429 and E433 whereas WH contacts with duplex DNA at positions T511 and Y564 on the bottom strand and at positions A525 and R528 on the top strand [22]. Previous structure reported that the WH of the RECQ1 contacts exclusively with ZBD with the helical hairpin presenting a flat surface underneath the D2 domain of the ATPase core [25]. In contrast, in *E. coli* RecQ, the WH contacts both the ZBD and the D1 domain [25]. Thus the interplay between the helicase domain and the WH domain of RECQ1 may be finely tuned by the ZBD to ensure precise DNA binding.

Homology modeling in molecular operating environment [42] shows that the four cysteine residues located on the loop of a side chain could act like a hinge to assist RECQ1

interaction with the DNA (Figure 9). While the cysteine residues at positions 453, 475 and 478 are located in the part of RECQ1 protein directly going down to interact with DNA (shown as green and yellow ribbon), cysteine 471 is located on the far end of the protein in a flexible loop which is separated by a strong interaction of cysteine 453 with zinc (Figure 9). Our data supports the cysteine residue 471 to be dispensable for zinc binding. Alteration of the conserved cysteine residues 453, 475 or 478 in RECQ1 led to the loss of zinc ion with incorrectly folded or partially denatured proteins sensitive to the proteolysis. This proteolytic pattern is coincident with the zinc-demetalated RECQ1 protein. Our thermal denaturation experiments showed high basal SYPRO Orange fluorescence even at low temperatures for RECQ1-C453A, RECQ1-C475A, and RECQ1-C478A, indicating that hydrophobic residues are exposed in these recombinant proteins. However the full-length RECQ1-WT and RECQ1-C471A proteins showed very similar thermal transition patterns with low initial florescence indicating that these proteins are probably folded in native manner where not many hydrophobic residues are exposed. Indeed, RECQ1-WT and RECQ1-C471A proteins displayed very similar pattern for helicase, ATPase, annealing activities and thermal denaturation curves. Moreover, the RECQ1-C471A protein was able to bind zinc ion to the similar level as the wild-type RECQ1 protein. Thus we conclude that ZBD is a crucial contributor to RECQ1's folding cascade, favoring the link between the domains and the overall protein's conformation to play a dual role in modulating the structural and functional state of the RECQ1 protein. Earlier reports have shown that RECQ1 is unusual among human RECQ proteins due to its quaternary structures. It is plausible that the altered conformational state of the mutant RECQ1 protein modulates its ability to process intermediates of DNA replication and repair that require coordinated unwinding and annealing activities of RECQ1. Future studies will test the impacts of these mutants on cellular functions of RECQ1 in DNA replication and repair.

Recurrent *RECQ1* mutations in two founder populations in Poland and Quebec, Canada, were found to significantly increase the risk of breast cancer [4]. The association of *RECQ1* mutations with breast cancer has been also confirmed in a Chinese population [5], suggesting that *RECQ1* mutations are not limited to a specific population. Single nucleotide polymorphisms (SNPs) in RECQ1 have also been associated with poor survival in pancreatic cancer patients receiving gemcitabine treatment [43]. Thus, RECQ1 variants may contribute to tumorigenesis, modify response to chemotherapy or act as genetic modifiers to influence pathogenesis [6]. The reported pathogenic mutations truncated or disrupted the RECQ1 protein or introduced missense mutations in its helicase and RQC domains [4,5]. Several RECQ1 variants including a synonymous SNP at C475 (rs142226004) reside in RQC domain adjacent to the conserved cysteine residues in the ZBD (http://www.ncbi.nlm.nih.gov/SNP/snp_ref.cgi?locusId=5965) and a missense (substitution) mutation, C453R, in the ZBD of RECQ1 is reported in a tumor sample (Uterine Corpus Endometrioid Carcinoma, TCGA-B5-A11O-01; http://cancer.sanger.ac.uk/cosmic/mutation/overview?id=937938). Missense mutations affecting the cysteine residues of the zinc-binding pocket of BLM have been reported in patients with Bloom Syndrome, a cancer predisposition disease [29]. Our efforts to engineer the corresponding mutated RECQ1 protein have been hampered due to the instability of the resultant protein; however, individual substitutions of cysteine residues in the ZBD predict potential molecular

consequences for the reported mutation in cancer. Overall, our results indicate that the zinc binding domain within the RQC domain is a key structural element that is essential for the structure-functions of RECQ1.

Acknowledgments

This work was funded by the NIGMS/NIH grant SC1GM093999 to SS and the ARO grant W911NF-15-1-0216 to RKG. We also acknowledge infrastructure support from the NIMHD/NIH under award number G12MD007597.

REFERENCES

1. Sharma S, Doherty KM, Brosh RM Jr. Biochem. J. 2006; 398:319–337. [PubMed: 16925525]
2. Croteau DL, Popuri V, Opresko PL, Bohr VA. Annu. Rev. Biochem. 2014; 83:519–552. [PubMed: 24606147]
3. Monnat RJ Jr. Semin. Cancer Biol. 2010; 20:329–339. [PubMed: 20934517]
4. Cybulski C, Carrot-Zhang J, Kluzniak W, Rivera B, Kashyap A, Wokolorczyk D, et al. Nat. Genet. 2015; 47:643–646. [PubMed: 25915596]
5. Sun J, Wang Y, Xia Y, Xu Y, Ouyang T, Li J, et al. PLoS Genet. 2015; 11:e1005228. [PubMed: 25945795]
6. Akbari MR, Cybulski C. Oncotarget. 2015; 6:26558–26559. [PubMed: 26387136]
7. Sami F, Sharma S. Comput. Struct. Biotechnol. J. 2013; 6:e201303014. [PubMed: 24688722]
8. Sharma S, Brosh RM Jr. Cell. Cycle. 2008; 7:989–1000. [PubMed: 18414032]
9. Sharma S, Brosh RM Jr. PLoS One. 2007; 2:e1297. [PubMed: 18074021]
10. Garige M, Sharma S. Int. J. Toxicol. 2014; 33:373–381. [PubMed: 25228686]
11. Sharma S, Phatak P, Stortchevoi A, Jasin M, Larocque JR. DNA Repair (Amst). 2012; 11:537–549. [PubMed: 22542292]
12. Sharma S, Stumpo DJ, Balajee AS, Bock CB, Lansdorp PM, Brosh RM Jr, et al. Mol. Cell. Biol. 2007; 27:1784–1794. [PubMed: 17158923]
13. Lu X, Parvathaneni S, Hara T, Lal A, Sharma S. Mol. Cancer. 2013; 12 29-4598-12-29.
14. Berti M, Ray Chaudhuri A, Thangavel S, Gomathinayagam S, Kenig S, Vujanovic M, et al. Nat. Struct. Mol. Biol. 2013; 20:347–354. [PubMed: 23396353]
15. Thangavel S, Mendoza-Maldonado R, Tissino E, Sidorova JM, Yin J, Wang W, et al. Mol. Cell. Biol. 2010; 30:1382–1396. [PubMed: 20065033]
16. Parvathaneni S, Stortchevoi A, Sommers JA, Brosh RM Jr, Sharma S. PLoS One. 2013; 8:e62481. [PubMed: 23650516]
17. Popuri V, Hsu J, Khadka P, Horvath K, Liu Y, Croteau DL, et al. Nucleic Acids Res. 2014; 42:5671–5688. [PubMed: 24623817]
18. Larsen NB, Hickson ID. Adv. Exp. Med. Biol. 2013; 767:161–184. [PubMed: 23161011]
19. Vindigni A, Marino F, Gileadi O. Biophys. Chem. 2010; 149:67–77. [PubMed: 20392558]
20. Cui S, Klima R, Ochem A, Arosio D, Falaschi A, Vindigni A. J. Biol. Chem. 2003; 278:1424–1432. [PubMed: 12419808]
21. Sharma S, Sommers JA, Choudhary S, Faulkner JK, Cui S, Andreoli L, et al. J. Biol. Chem. 2005; 280:28072–28084. [PubMed: 15899892]
22. Pike AC, Gomathinayagam S, Swuec P, Berti M, Zhang Y, Schnecke C, et al. Proc. Natl. Acad. Sci. U.S.A. 2015; 112:4286–4291. [PubMed: 25831490]
23. Muzzolini L, Beuron F, Patwardhan A, Popuri V, Cui S, Niccolini B, et al. PLoS Biol. 2007; 5:e20. [PubMed: 17227144]
24. Vindigni A, Hickson ID. HFSP J. 2009; 3:153–164. [PubMed: 19949442]
25. Pike AC, Shrestha B, Popuri V, Burgess-Brown N, Muzzolini L, Costantini S, et al. Proc. Natl. Acad. Sci. U.S.A. 2009; 106:1039–1044. [PubMed: 19151156]
26. Kitano K. Front. Genet. 2014; 5:366. [PubMed: 25400656]

27. Banerjee T, Sommers JA, Huang J, Seidman MM, Brosh RM Jr. Curr. Biol. 2015; 25:2830–2838. [PubMed: 26455304]
28. Liu JL, Rigolet P, Dou SX, Wang PY, Xi XG. J. Biol. Chem. 2004; 279:42794–42802. [PubMed: 15292213]
29. Guo RB, Rigolet P, Zargarian L, Fermandjian S, Xi XG. Nucleic Acids Res. 2005; 33:3109–3124. [PubMed: 15930159]
30. Gyimesi M, Harami GM, Sarlos K, Hazai E, Bikadi Z, Kovacs M. Nucleic Acids Res. 2012; 40:3952–3963. [PubMed: 22253018]
31. Brosh RM Jr, Opresko PL, Bohr VA. Methods Enzymol. 2006; 409:52–85. [PubMed: 16793395]
32. Ren H, Dou SX, Zhang XD, Wang PY, Kanagaraj R, Liu JL, et al. Biochem. J. 2008; 412:425–433. [PubMed: 18290761]
33. Marin MS, Casais R, Alonso JM, Parra F. J. Virol. 2000; 74:10846–10851. [PubMed: 11044135]
34. Niesen FH, Berglund H, Vedadi M. Nat. Protoc. 2007; 2:2212–2221. [PubMed: 17853878]
35. Hunt JB, Neece SH, Ginsburg A. Anal. Biochem. 1985; 146:150–157. [PubMed: 3887984]
36. Sami F, Lu X, Parvathaneni S, Roy R, Gary RK, Sharma S. Biochem. J. 2015; 468:227–244. [PubMed: 25774876]
37. Brosh RM Jr, Sharma S. Methods Mol. Biol. 2006; 314:397–415. [PubMed: 16673896]
38. Doherty KM, Sharma S, Uzdilla LA, Wilson TM, Cui S, Vindigni A, et al. J. Biol. Chem. 2005; 280:28085–28094. [PubMed: 15886194]
39. Wu Y. J. Nucleic Acids. 2012; 2012:140601. [PubMed: 22888405]
40. Jerabek-Willemsen M, Wienken CJ, Braun D, Baaske P, Duhr S. Assay Drug Dev. Technol. 2011; 9:342–353. [PubMed: 21812660]
41. Wu Y, Brosh RM Jr. DNA Repair (Amst). 2010; 9:315–324. [PubMed: 20061189]
42. Molecular operating environment (MOE), 2013.08. 1010 sherbooke st. west, suite #910, montreat, QC, canada, H3A, 2R7, 2015: Chemical Computing Group Inc;
43. Li D, Frazier M, Evans DB, Hess KR, Crane CH, Jiao L, et al. J. Clin. Oncol. 2006; 24:1720–1728. [PubMed: 16520463]

Highlights

- The zinc binding motif in the RQC domain of RECQ1 is a key structural element.
- Cysteine residues that coordinate zinc are critical for the RECQ1 ATPase and helicase activities.
- RECQ1 mutants that lack zinc binding retained DNA binding and annealing activities.
- Conserved cysteine residues contribute differentially to the RECQ1 structure and functions.

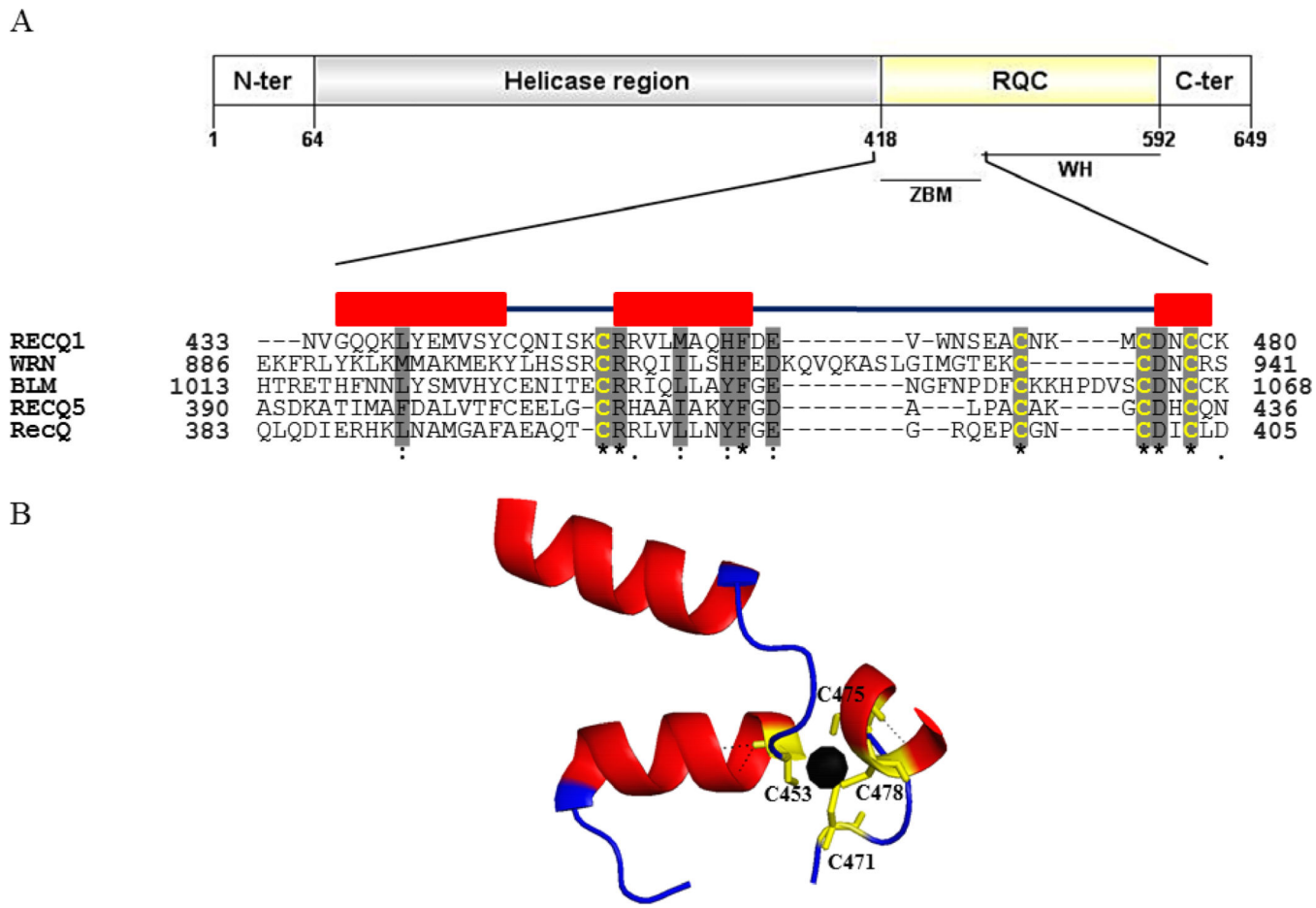

Figure 1. Schematic representation of RECQ1 protein

(A) Conserved domains in RECQ1 and amino acid sequence alignment of the conserved zinc binding domain (ZBD) among the RecQ family helicases in humans. The multiple sequence alignments were generated with MUSCLE and refined manually. Positions of the first and the last amino acid residues are shown by the numbers at the beginning and end of each sequence, respectively. Highly conserved residues are shadowed in gray color. In bold yellow color are the four conserved cysteine residues. Secondary structure elements of the RECQ1 are shown with boxes designating the α-helices. (B) Ribbon drawing of the ZBD of the crystallized truncated RECQ1 protein (PDB ID: 4U7D). The zinc ion shown as a black sphere is coordinated by four conserved cysteine residues.

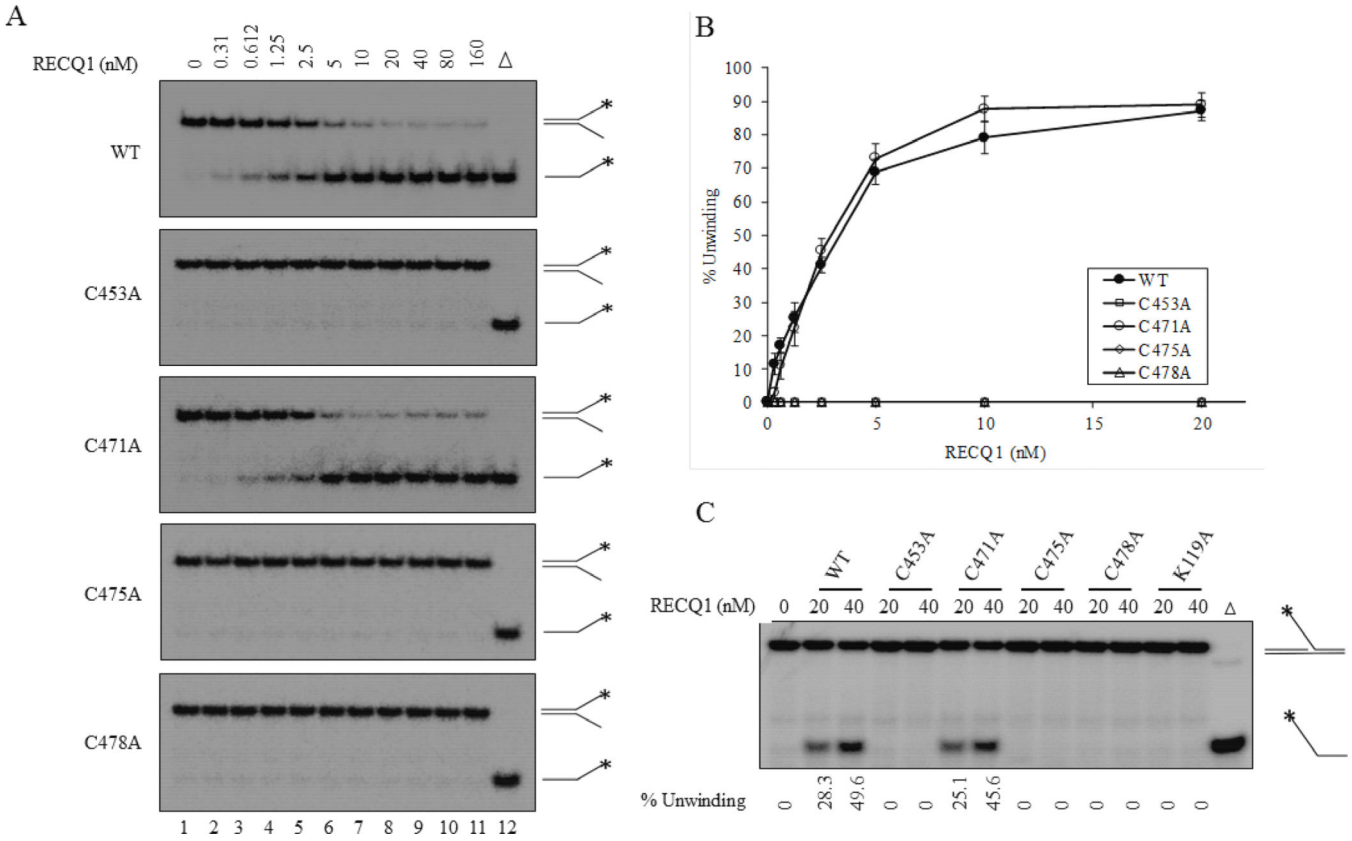

Figure 2. DNA unwinding activity of ZBD mutants of RECQ1

(A) Increasing concentrations of indicated RECQ1 proteins were incubated with a radiolabelled 19-bp fork duplex DNA substrate (0.5 nM) in a standard helicase assay. Reaction mixtures were incubated for 30 min at 37°C, followed by proteinase K treatment, and subsequently loaded on to native 12 % polyacrylamide gels. (B) Quantitative comparison of helicase activity of wild-type and cysteine mutants on fork duplex substrate. The results shown are the average of at least three independent experiments, with SDs indicated by error bars. (C) Unwinding of a 26 nt 5'-flap DNA substrate. Each protein, either 20 nM or 40 nM, was incubated with radiolabelled FLAP DNA substrate (0.5 nM) in a standard helicase assay. Percent unwinding in each reaction is indicated.

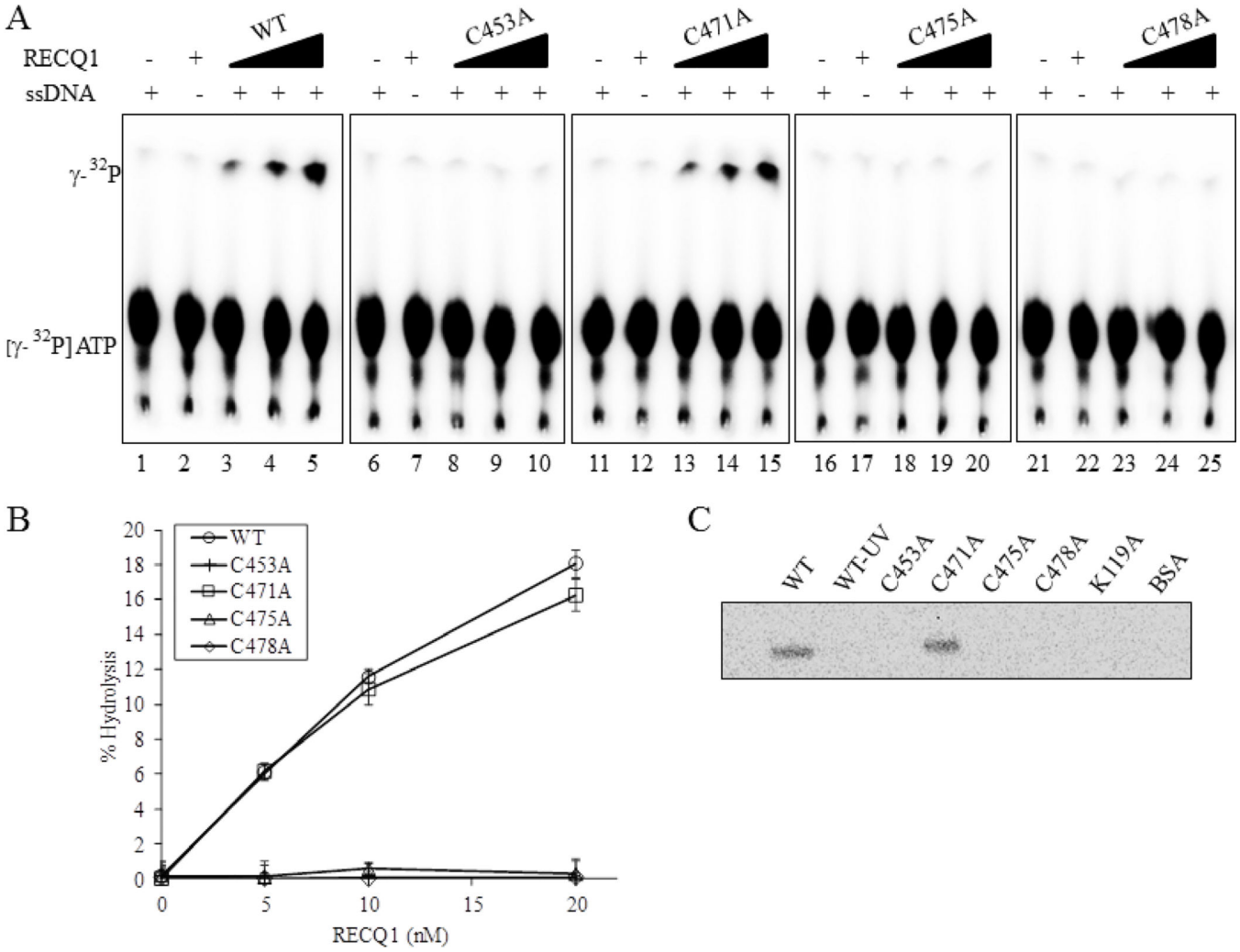

Figure 3. ZBD mutants RECQ1-C453A, RECQ1-C475A and RECQ1-C478A are ATPase deficient

(A) Representative thin-layer chromatography showing dose-dependent ATPase activity of wild-type and ZBD mutants of RECQ1. RECQ1 proteins (5, 10 and 20 nM) in ATPase assay mixture containing radiolabelled γP^{32}-ATP, cold ATP in the absence or presence of single strand DNA were incubated for 30 min at 37°C followed by autoradiography. Lanes 1, 6, 11, 16, 21 are no enzyme controls; lanes 2,7,12, 17, 22 are no single strand DNA controls. (B) Quantitative comparison of ATPase activity of wild-type and cysteine mutants. The average values are presented with SDs indicated by error bars from triplicate assays. (C) ATP binding activity of wild-type and mutant RECQ1 proteins. One microgram of the wild-type or mutant helicase protein was incubated with [γ-^{32}P] ATP in the presence of fixed concentration of single strand DNA and increasing concentrations of proteins was UV cross-linked as described in Materials and Methods. Following SDS-PAGE electrophoresis, gel was visualized using a PhosphorImger.

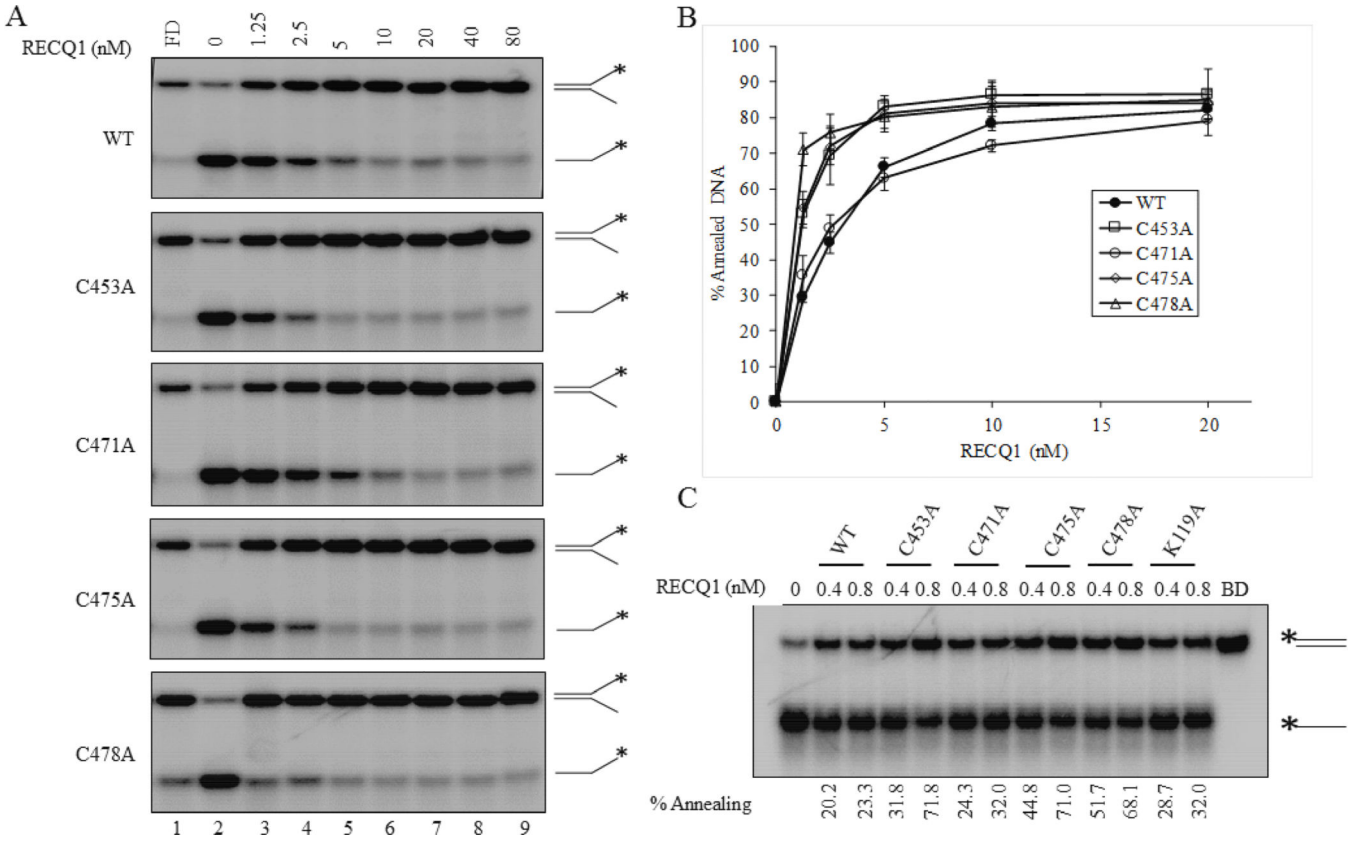

Figure 4. DNA strand-annealing activity of ZBD mutants of RECQ1

(A) RECQ1 concentration dependent strand-annealing of partially complementary single strand DNA to generate a 19-bp forked duplex in the absence of ATP. Lane 1, No enzyme; lanes 2–8, RECQ1-WT or mutant at indicated concentration; lane 9, fork duplex marker (FD). (B) Quantitative comparison of strand-annealing activity of wild-type and cysteine mutants to generate fork duplex product. The results shown are the average of at least three independent experiments, with SDs indicated by error bars. (C) Concentration-dependent strand-annealing activity of wild-type and ZBD variants using fully complementary single strand DNA molecules to generate a blunt duplex product. Each protein, either 0.4 nM or 0.8 nM, was incubated with radiolabelled T44 oligo and unlabeled T44-RC oligo in the absence of ATP. Blunt duplex (BD) marker is shown in the last lane. Percent annealing in each reaction is indicated.

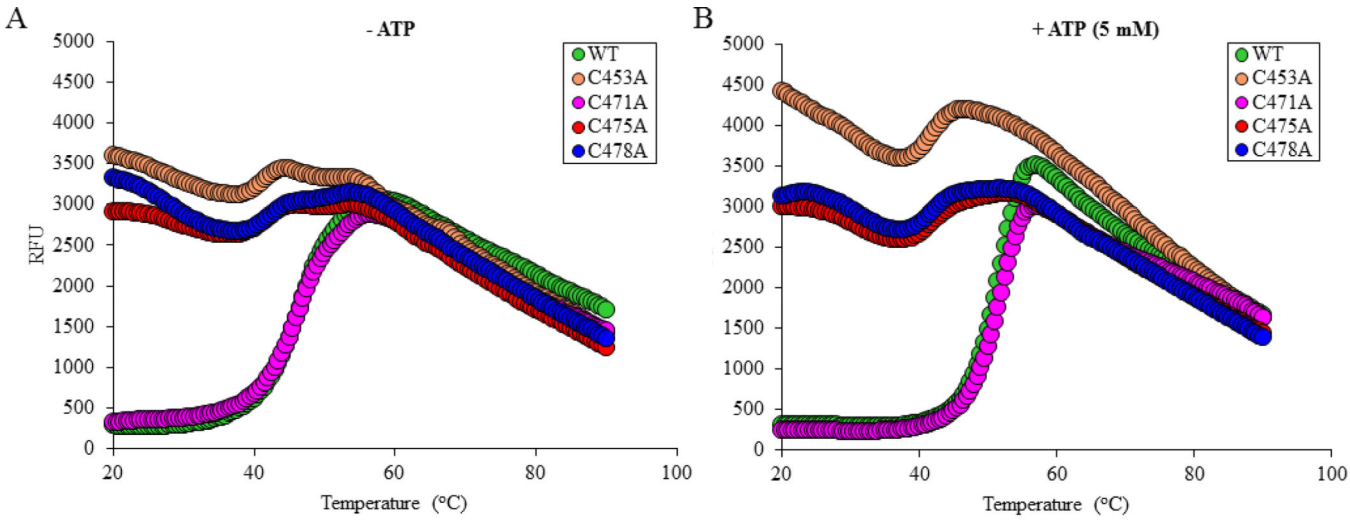

Protein	Tm (°C)	
	-ATP	-ATP
RECQ1-WT	46 ± 0.04	52 ± 0.04
RECQ1-C453A	41 ± 0.06	42 ± 0.05
RECQ1-C471A	47 ± 0.04	52 ± 0.8
RECQ1-C475A	43 ± 0.9	42 ± 0.07
RECQ1-C478A	41 ± 0.08	42 ± 0.06

Figure 5. Thermal stability of ZBD mutants of RECQ1 in the absence (A) or presence (B) of 5 mM ATP

Thermal melting curves for wild-type and mutants are shown, along with calculated melting temperature (T_m). Assays were performed in a 20 μL reaction containing 10 μM wild-type or mutant protein mixed with SYPRO Orange in 50 mM HEPES-NaOH, pH 8.0, 60 mM NaCl, 1 mM DTT and 15 % (v/v) glycerol, with or without 5 mM ATP. The T_m was calculated from the maximum value of the negative first derivative of fluorescence intensity versus temperature; this is approximately the midpoint of the unfolding transition.

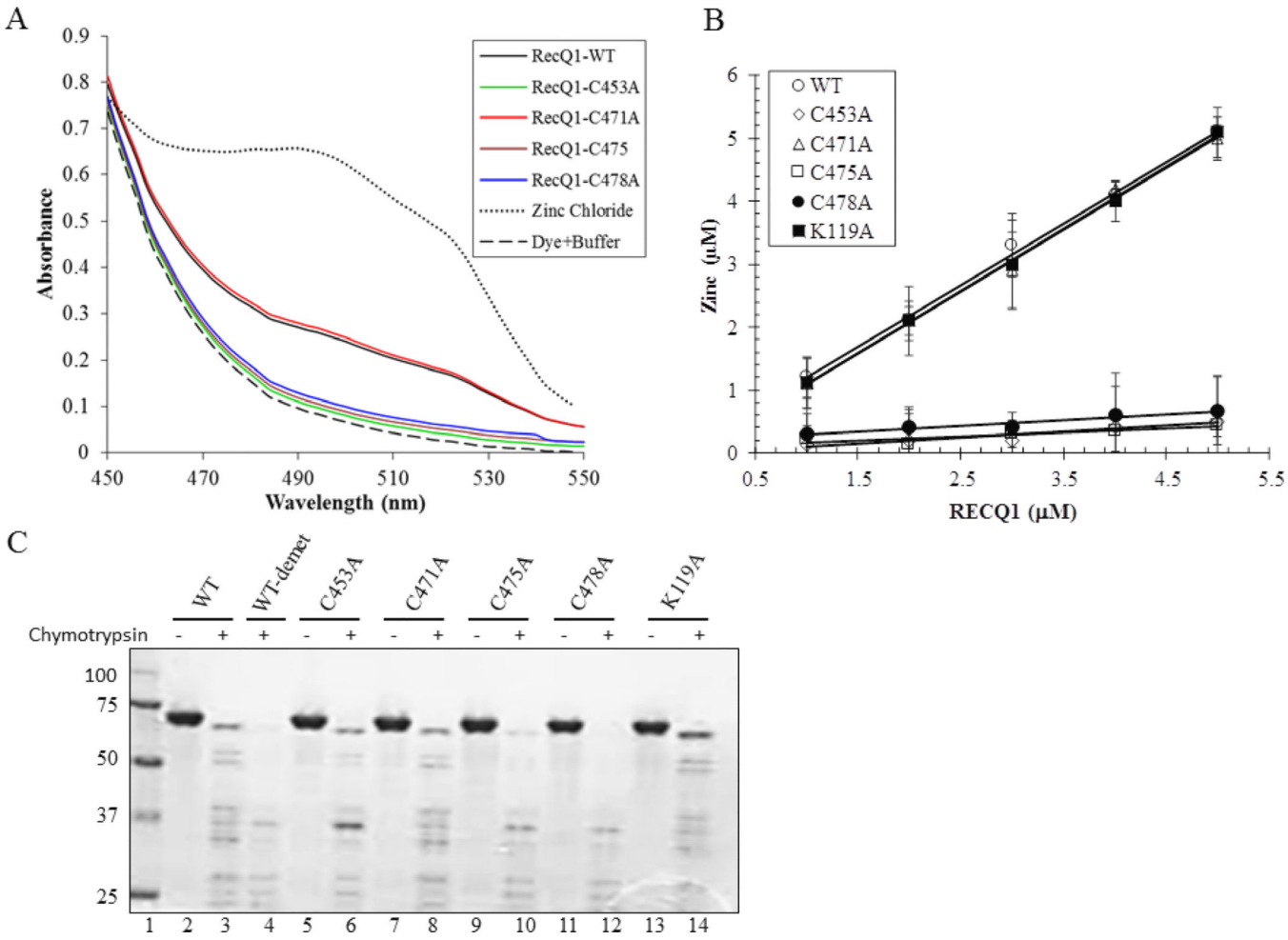

Figure 6. Quantification of zinc bound to wild-type and ZBD mutants of RECQ1

(A) Absorbance spectra of RECQ1-WT and mutant proteins in the presence of PAR (100 μM). The spectra were scanned from 300 to 600 nm. 20 nM $ZnCl_2$ was utilized as control and scanned in the same conditions. All assays were performed at 25°C. (B) Quantity of the zinc ion was determined with increasing concentration of the protein. The slope value of 0.97–0.99 for RECQ1-WT and RECQ1-C471A indicates that zinc ion binds to the protein in a 1:1 stoichiometric ratio. (C) Partial proteolytic digestion of wild-type and ZBD mutants. RECQ1 proteins were incubated with chymotrypsin (enzyme substrate ratio to 1:100) in a 20 μL reaction mixture as described in Materials and Methods. Samples were quenched after 10 min, separated by SDS-PAGE, and stained with Coomassie Blue. The molecular mass standards (kDa) are shown on the left in lane 1.

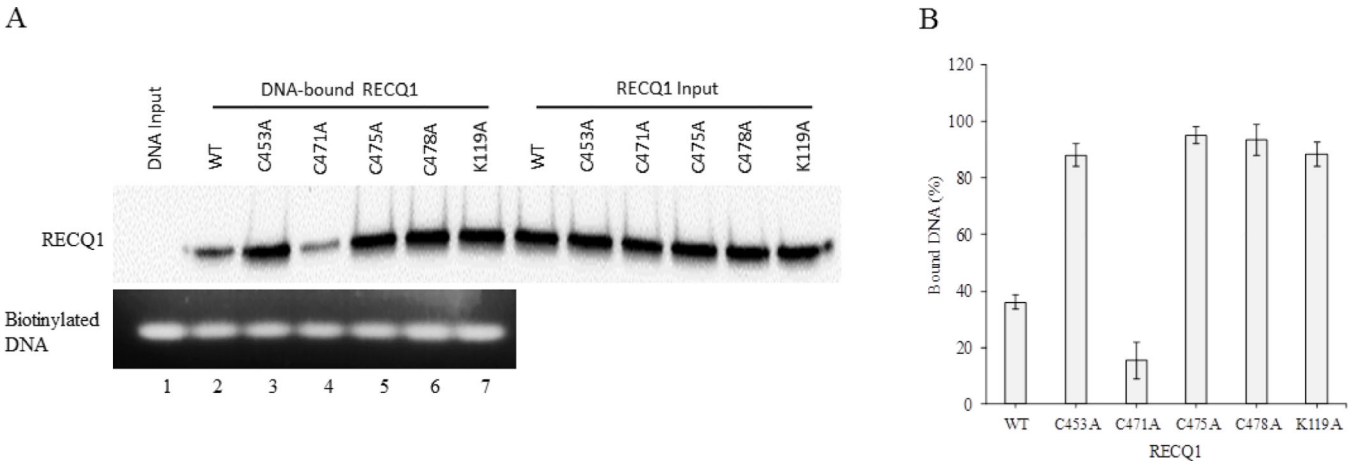

Figure 7. ZBD mutants RECQ1-C453A, RECQ1-C475A and RECQ1-C478A display strong DNA binding activity

(A) Binding reactions were performed using biotinylated DNA probe and 100 nM of wild-type or each mutant RECQ1 protein. The DNA-protein complexes were pulled-down on streptavidin magnetic beads and DNA-bound proteins were analyzed by Western blotting. *Top:* Western blot analysis for wild-type and each mutant. *Bottom:* Comparable amount of DNA was pulled-down in all reactions as shown by agarose gel analyses. Lane 1 represents biotinylated DNA bound to the streptavidin beads in the absence of RECQ1 variants. (B) Quantitation of the Western blot using ImageJ and represented as mean with SD from at least three experiments.

A

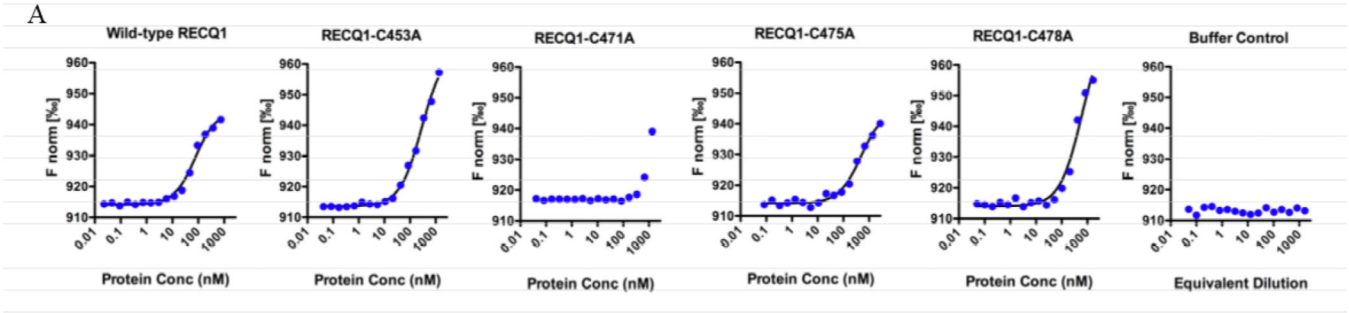

B

RECQ1 Protein	K_d (nM)
Wild-type	**66 ± 10**
C453A	**276 ± 27**
C471A	**≥ 1000**
C475A	**473 ± 78**
C478A	**602 ± 152**

Figure 8. Measurement of dissociation constant using microscale thermophoresis (MST)

Fluorescently-labeled forked duplex DNA (20 nM) was mixed with 2-fold serial dilutions of protein and analyzed by MST. The proteins were diluted in MST binding buffer to give final concentrations of 0.02–750 nM for wild-type RECQ1, 0.04–1370 nM for C453A, 0.04–1350 nM for C471A, 0.08–2730 nM for C475A, and 0.05–1650 nM for C478A. As a control, protein storage buffer was serially diluted with MST binding buffer and analyzed. The MST signal was plotted versus the log of the protein concentration, and the data were fit to a non-cooperative binding model to estimate K_d.

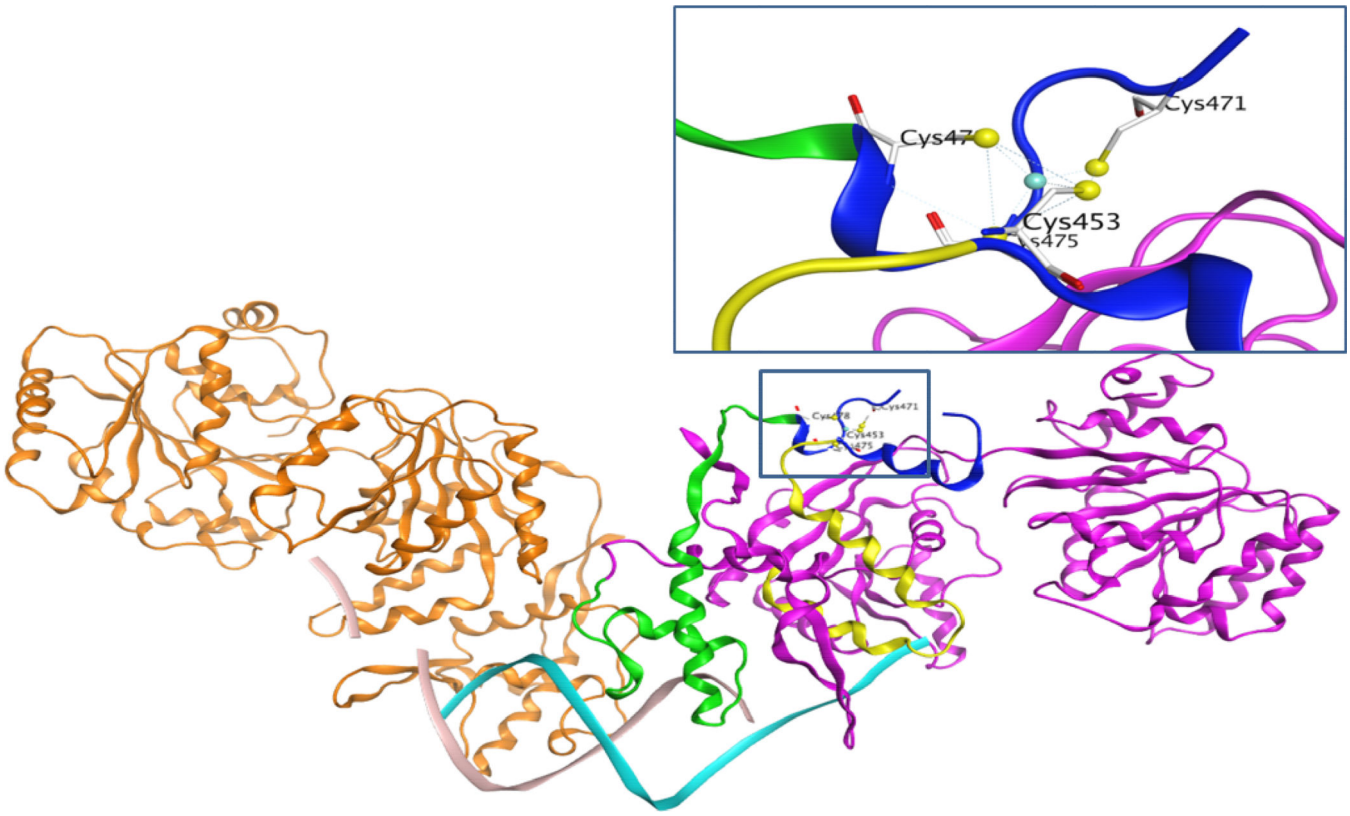

Figure 9. Differential contribution of conserved cysteine residues in RECQ1 structure and function

Homology modeling shows that the four cysteine residues located on the loop of a side chain could act like a hinge to assist RECQ1 interaction with the DNA. Cysteine residues 453, 475, and 478 are located on the part of RECQ1 protein shown as the ribbon highlighted green and yellow. These parts of the protein are directly going down to interact with DNA, indicating a major contribution for a specific protein conformation and DNA binding activity. On the other hand, the cysteine 471 is located on the far end of the protein in a flexible loop, and one end of the loop is separated by a strong interaction of cysteine 453 with zinc. The newly solved crystal structure of the truncated RECQ1 protein (PDB ID: 4U7D) did not show data for this loop, perhaps due to its intrinsically unstructured character.

Table 1

Oligonucleotide sequences for various DNA substrates (5’-3’)

Name	Length (nt)	Sequence
T44	44 GCACTGGCCGTCGTTTTACGGTCGTGACTGGGAAAACCCTGGCG	
T44-RC	44CGCCAGGGTTTTCCCAGTCACGACCGTAAAACGACGGCCAGTGC	
FUS25	25	CGCCAGGGTTTTCCCAGTCACGACC
FLAP26	45TTTTTTTTTTTTTTTTTTTTTTCCAAGTAAAACGACGGCCAGTGC	